

Evaluation of the Structural Fragility of a Bridge Structure Subjected to a Tsunami Wave Load

Gaku SHOJI and Tetsuo MORIYAMA

Department of Engineering Mechanics and Energy, Graduate School of Systems and Information Engineering, University of Tsukuba

(Received for 1 June., 2007 and in revised from 24 Oct, 2007)

ABSTRACT

In this study, the structural fragility of a bridge structure due to a tsunami wave load is evaluated, quantitatively analyzing the damage data of bridge structures due to the 2004 Tsunami in Sri Lanka and in Indonesia, which are on basis of 58 data on Sri Lanka and 17 data on Sumatra. By the formulation of a fragility curve of a bridge structure from statistical analysis of the data, the structural fragility of a bridge structure due to a tsunami wave load, which describes the relation between the tsunami damage classification of a bridge structure and a tsunami wave load such as inundation depth and inundation height, is revealed.

1. INTRODUCTION

A giant earthquake of M 9.1, whose hypocenter was located far off the northern part of Sumatra island in Indonesia, occurred on December 26th, 2004 (UTC 00:58:53) (USGS, 2007). The tsunami induced by the earthquake caused catastrophic damage in countries surrounding the Indian Ocean such as Indonesia, Sri Lanka, Thai, India, Malaysia, and Myanmar. The main reason for the damage is that as well as masonry and wooden houses necessary for the dairy life of inhabitants being severely affected by tsunami wave loads, infrastructure such as transportation facilities, electricity power supply systems, and water treatments were also affected structurally and functionally. For instance, along the east, south, and southwest coastline of Sri Lanka of a total about 1,000 km, and along the northwest coastline of Sumatra of more than 250 km, road infrastructure was affected by the tsunami, and various damage patterns, which are classified into washout and movement of a superstructure, minor damage, and scouring and erosion of soil embankments around abutments, were observed dependent on the tsunami wave height.

Such infrastructure systems play a crucial role for the stakeholders involved in a tsunami disaster in responding at the stage of crisis management even after an event as well as in reconstruction and rehabilitation management; it is important to use road infrastructure for the evacuation of inhabitants and first-aid for wounded persons, for transportation of emergency materials to affected areas, and for dispatch of associated expertise at the above stages. In consideration of the high risk associated with a tsunami disaster in Japan that is feared with the anticipated Tokai, Tohankai, and Nankai Earthquake, the development of a framework of tsunami risk assessment for infrastructure is significantly required.

Many valuable studies on the fragility evaluation of a structure due to a tsunami have been conducted mainly in the field of seismology as well as and coastal and hydraulic engineering. Among

these, Hatori (1984) clarified the relation between the damage percentage of a wooden house with an inundation height on the basis of previous tsunami damage data such as the 1933 Sunriku and the 1960 Chile Tsunamis, and Shuto (1993) first introduced the tsunami fragility curve of a wooden house based on analysis of the results by Hatori (1984). Matsutomi and Shuto (1994) analyzed the relation between the damage level of a reinforced concrete (RC) house, a concrete bloc house, and a wooden house with an inundation height from assessment of tsunami damage data of the 1993 Hokkaido-Nanseioki Earthquake. From the viewpoint of evaluation of tsunami wave velocity, which is the other important index of a tsunami wave load, Matsutomi and Iizuka (1998) theoretically formulated equations to evaluate tsunami wave velocity on basis of the results of their hydraulic experiments. In addition, from the viewpoint of evaluation of tsunami wave force on a structure, Matsutomi and Oomukai (1999) evaluated the drag force acting on a house on the basis of a series of hydraulic experiments. Mizutani and Imamura (2000) showed a framework of evaluation of tsunami wave pressure on an inclined structure such as a shore protection structure, and Asakura et al. (2000) proposed a model to describe tsunami wave pressure on a structure when a tsunami runs up across a shore protection structure. Furthermore, experimental and numerical studies were conducted to clarify the hydrodynamic force acting on a house in groups of houses due to flood- or tsunami- induced flow (Fukuoka et al., 1997, Iizuka and Matsutomi, 2000). However, these researchers dealt with tsunami wave loads affecting houses and costal infrastructure such as a shore protection structure, whereas there is insufficient research dealing with tsunami damage to road infrastructure, although results on the basis of a field survey of road structures in Indonesia and in Sri Lanka were promptly reported even after the 2004 Tsunami in the Indian Ocean (e.g., Iemura et al., 2005, Unjho et al., 2005, Shoji and Mori, 2006, Kosa et al., 2006).

For the reason above, in this study, the structural fragility of a

bridge structure due to a tsunami wave load is evaluated, quantitatively analyzing the damage data of bridge structures due to the 2004 Tsunami in Sri Lanka and in Indonesia, on the basis of 58 data on Sri Lanka and 17 data on Sumatra. From the statistical analysis, the relation between the probability of tsunami damage to a bridge structure to a tsunami wave load such as the inundation depth and the inundation height is revealed.

2. FRAGILITY CURVE

Failure probability P_f of a bridge structure due to a tsunami is derived as probability $P(C \leq R)$ so that the response of a bridge due to a tsunami R (bridge response) becomes equal to and larger than the resistance of a bridge against a tsunami C (bridge resistance) as follows:

$$P_f = P(C \leq R) = P\left(X = \frac{C}{R} \leq 1.0\right) \quad (1)$$

where R is the function $R(r_m, \delta_r)$ of median r_m and coefficient of variation δ_r of the bridge response, and C is the function of $C(c_m, \delta_c)$ of median c_m and coefficient of variation δ_c of the bridge resistance. X is the random variable to present the ratio of bridge resistance C to bridge response R , and then X is assumed to be logarithmic normal distribution. Hence, probability density function f_x associated with X is derived as follows:

$$f_x = \frac{1}{\sqrt{2\pi} \cdot \xi \cdot x} \exp\left[-\frac{1}{2} \left\{ \frac{\ln x - (\ln c_m - \ln r_m)}{\xi} \right\}^2\right] \quad (2)$$

where ξ is the logarithmic standard deviation:

$$\xi = \sqrt{\ln(1 + \delta_c^2)(1 + \delta_r^2)}$$

From Eq. (1) and Eq. (2), failure probability P_f of a bridge structure due to a tsunami is derived as probability distribution function F_x of f_x as follows:

$$P_f = F_x = \int_0^1 \frac{1}{\sqrt{2\pi} \cdot \xi \cdot x} \exp\left[-\frac{1}{2} \left\{ \frac{\ln x - (\ln c_m - \ln r_m)}{\xi} \right\}^2\right] dx \quad (3)$$

Now, the variable transformation associated with X is performed as the following Eq. (4), and random variable Z is newly defined as a parameter in order to calibrate the dimension of X by multiplying X by median r_m of bridge response R and to make Z the same dimension as C :

$$Z = X \cdot r_m = \frac{C}{R} \cdot r_m \quad (4)$$

Substituting Eq. (4) for Eq. (3), failure probability P_f of a bridge structure due to a tsunami is derived as the function of C :

$$P_f = F_z(r_m) = \int_0^{r_m} \frac{1}{\sqrt{2\pi} \cdot \xi \cdot z} \exp\left[-\frac{1}{2} \left\{ \frac{\ln z - \ln c_m}{\xi} \right\}^2\right] dz \quad (5)$$

By the modification of Eq. (5), the damage probability of a bridge structure in relation to a tsunami wave load will be modeled mathematically as a fragility curve as shown in the following chapter.

3. TSUNAMI FRAGILITY ASSESSMENT OF A BRIDGE STRUCTURE

3.1 SUBJECT DATA

(1) DAMAGE DATA OF BRIDGE STRUCTURES IN SRI LANKA

Subject data used for fragility analysis are the damage data of bridge structures collected in Sri Lanka by Shoji and Mori (2006). These bridges are located along the southwest and south coast of Sri Lanka as shown in Fig. 1. Shoji and Mori (2006) collected and archived 60 data that contain the information shown in Table 1: the structural failure mode of subject bridges due to a tsunami, structural type, bearing type, span, length of deck, height of deck, total width of deck, thickness of deck, distance from the coastline to a subject bridge, the height from the still water surface level under the bridge to the deck, and the inundation depth around a subject bridge due to a tsunami. Based on the data, we classified the damage pattern of affected bridges from washout and fall-down of a deck (rank A), movement of a deck or damage to an abutment due to scouring and erosion (rank B), minor damage to a deck attachment such as bridge railings (rank C), to no damage (rank D) as shown in Table 2.

Fig. 2 shows the structural type, span, and bearing type of subject bridges and Fig. 3 shows a schematic view of two affected bridges, Akurala Bridge in Paraliya and Magalle Bridge in Galle City, to introduce rank A and rank B damage to one of the bridges in Sri Lanka. A quantitative index to present a tsunami wave load on a bridge structure in mechanics is the inundation depth around a subject bridge as previously mentioned. The value of an inunda-

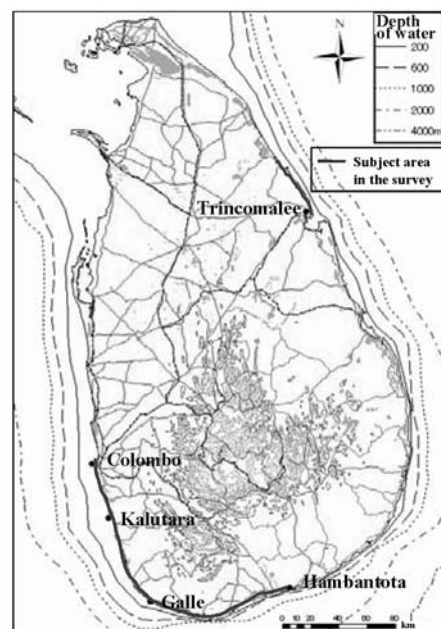


Fig. 1 Subject road infrastructure in Sri Lanka

Table 1 Structural characteristics and failure mode of subject bridges, and data on inundation depth around subject bridges in Sri Lanka

Number	Name of bridge	District	Latitude	Longitude	Structural type	Type of bearing	Distance from coastline (m)	Total length of deck (m)	Distance from water surface to deck (m)	Length of span (m)	Width of deck (m)	Height of deck (m)	Inundation depth (m)	Measured or Hearing	Damage rank
1	Bolgoda Bridge	Moratuwa	N6°43'37.3"	E79°54'12.6"	10span PC	Rubber pad type	1000	190.93	1.43	19.09	15.54	1.50	1.43	Hearing	B
2	Talpitaya Bridge	Pansudra	N6°41'02.9"	E79°55'12.2"	2span PC	Rubber pad type	500	43.13	3.58	21.56	12.15	1.94	1.22	Hearing	D
3	Kalutara Bridge	Kalutara	N6°35'25.7"	E79°57'34.1"	6span PC	Rubber pad type	-	194.75	1.29	32.46	16.96	1.80	1.29	Hearing	D
4	Dumala Modara Bridge	Maggona	N6°30'38.5"	E79°58'55.3"	3span RC	Without bearing	105	23.88	0.85	7.96	12.80	1.00	6.39	Hearing	D
5	Maggona Bridge	Maggona	N6°29'55.6"	E79°58'51.0"	1span PC	Without bearing	97	22.00	1.31	22.00	13.31	1.40	7.91	Hearing	D
6	Ba-1	Beruwala	N6°27'53.9"	E79°59'13.6"	1span RC	Without bearing	-	5.10	0.55	5.10	9.49	0.40	-	-	D
7	Mogollia Custom Bridge	Beruwala	N6°28'20.1"	E79°58'48.0"	1span RC	Without bearing	120	16.79	1.00	16.79	8.28	1.10	4.39	Measured	C
8	Kaluwa Modara Bridge	North of Bentota	N6°26'32.5"	E79°59'33.0"	3span RC	Without bearing	106	48.04	1.58	16.01	15.25	1.80	1.58	Hearing	D
9	Bentota Bridge	Bentota	N6°25'35.7"	E79°59'54.6"	2span steel truss	Pin	218	91.00	3.30	45.50	7.10	-	3.43	Hearing	D
10	Athuruwella Bridge	Ambalangoda	N6°25'35.7"	E79°59'54.6"	1span RC	Without bearing	86	52.97	3.20	13.24	11.87	0.93	5.44	Hearing	D
11	Doowa Modara Bridge	Jandruwa	N6°20'37.0"	E80°01'32.1"	1span RC	Without bearing	201	16.19	1.12	16.19	14.44	1.10	4.19	Hearing	D
12	Jandruwa Bridge	Jandruwa	N6°20'29.1"	E80°01'35.6"	1span RC	Without bearing	168	9.82	1.33	9.82	13.94	0.75	2.59	Measured	D
13	Balpitaya Main Bridge	Balpitaya	N6°16'23.1"	E80°02'21.4"	3span RC	Without bearing	177	54.51	1.91	18.17	16.15	1.16	3.94	Hearing	B
14	Urawatte Bridge	Ambalangoda	N6°13'43.6"	E80°03'15.6"	2spans RC	Without bearing	58	32.50	3.89	16.25	16.15	1.10	6.04	Hearing	D
15	Akurala Bridge	Paraliya	N6°11'50.1"	E80°03'48.3"	2span RC	Without bearing	20	23.91	2.31	11.95	10.65	0.92	8.06	Hearing	A
16	Totagamawa Bridge	Hikkaduwa	N6°08'51.5"	E80°05'57.5"	3span RC	Without bearing	97	29.38	1.61	9.79	16.17	0.75	6.97	Hearing	D
17	H1-2	Hikkaduwa	N6°08'19.7"	E80°05'58.6"	1span RC	Without bearing	25	7.02	1.59	7.02	11.08	0.20	6.37	Hearing	B
18	H1-1	Hikkaduwa	N6°07'59.2"	E80°06'02.4"	1span RC	Without bearing	37	5.50	1.91	5.50	11.09	0.37	7.11	Hearing	B
19	Do-2	Dondruwa	N6°04'48.2"	E80°09'02.4"	1span culvert	Without bearing	20	2.28	0.90	2.28	12.33	0.33	3.02	Measured	B
20	Do-1	Dondruwa	N6°04'59.9"	E80°08'53.7"	1span RC	Without bearing	83	2.40	1.50	2.40	9.80	0.40	1.31	Measured	D
21	Dodanduwa Bridge	Dodanduwa	N6°06'16.9"	E80°07'32.0"	5span RC	Without bearing	126	52.98	2.29	10.60	17.81	0.77	3.54	Measured	B
22	Ba-2	Boosa	N6°04'40.9"	E80°09'07.8"	1span RC arch	Without bearing	87	2.30	0.76	2.30	9.20	0.30	4.98	Hearing	B
23	Ba-1	Boosa	N6°04'36.0"	E80°09'15.9"	1span brick	Without bearing	33	1.73	0.80	1.73	9.20	0.90	4.14	Hearing	B
24	Gintola Main Bridge	Gintola	N6°03'48.5"	E80°10'29.7"	5span PC	Without bearing, concrete bearing base	162	122.28	2.24	24.46	15.64	1.76	2.37	Hearing	D
25	Gintola Small Bridge	Gintola	N6°03'39.6"	E80°10'36.6"	1span RC	Rubber pad type	148	12.88	1.91	12.88	15.44	0.85	4.04	Measured	B
26	Maha Modara Bridge	Galle	N6°02'25.7"	E80°11'59.1"	3span RC	Without bearing	170	69.74	3.23	23.25	15.79	1.25	6.62	Hearing	C
27	Ga-1	Galle	N6°01'58.2"	E80°12'53.0"	2span RC arch	Without bearing	118	16.26	2.60	8.13	17.08	0.70	6.71	Hearing	C
28	Maggalle Bridge	Galle	N6°02'07.1"	E80°13'55.0"	1span RC	Without bearing	188	19.12	1.93	19.12	15.82	1.10	6.01	Hearing	B
29	Walgal Modara Bridge	Galle	N6°01'38.4"	E80°14'37.6"	3span RC	Without bearing	148	37.20	1.83	12.40	11.45	0.95	5.15	Hearing	C
30	Mih-3	Mihiripanna	N6°00'02.2"	E80°15'48.9"	1span RC	Without bearing	66	5.02	1.05	5.02	5.40	0.80	3.79	Hearing	A
31	Mih-2	Mihiripanna	N6°00'01.7"	E80°15'49.5"	1span RC	Without bearing	43	2.58	0.17	2.58	9.40	1.18	3.79	Hearing	D
32	Mih-1	Mihiripanna	N5°59'58.1"	E80°16'23.2"	1span RC	Without bearing	73	3.44	1.05	3.44	11.26	1.22	3.74	Hearing	D
33	Thimbiri Culvert	Koggala	N5°59'39.7"	E80°17'53.3"	3span RC arch	Without bearing	72	20.53	1.78	-	14.30	1.35	1.74	Hearing	D
34	Kog-1	Koggala	N5°59'03.3"	E80°19'53.4"	1span RC	Without bearing	51	2.00	0.75	2.00	9.87	0.64	4.44	Hearing	D
35	Katuluwa Main Bridge	Katuluwa	N5°58'58.4"	E80°20'09.6"	3span RC	Without bearing	119	49.32	1.93	16.44	18.80	1.80	5.46	Hearing	B
36	Ka-1	Katuluwa	N5°58'50.6"	E80°20'30.2"	1span RC arch	Without bearing	22	4.18	0.75	4.18	16.60	1.28	4.17	Hearing	D
37	Mi-1	Midigama	N5°58'31.9"	E80°21'18.9"	1span RC arch	Without bearing	29	4.60	0.79	4.60	10.35	0.84	4.00	Hearing	D
38	Ahangama Small Bridge	Ahangama	N5°58'10.8"	E80°22'07.7"	1span RC	Without bearing	15	8.46	2.03	8.46	7.00	0.78	6.54	Hearing	A
39	Goviyapana Bridge	Midigama	N5°57'56.1"	E80°22'57.5"	3span RC	Without bearing	92	49.05	1.64	16.35	12.13	1.00	3.89	Hearing	B
40	Midigama Bridge	Weligama	N5°57'50.7"	E80°23'06.6"	1span RC	Without bearing	45	11.03	1.95	11.03	8.40	0.75	9.38	Hearing	D
41	We-1	Weligama	N5°57'16.0"	E80°25'34.3"	1span culvert	Without bearing	32	8.37	2.22	8.37	17.52	0.73	6.29	Hearing	B
42	Polwattha Modara Bridge	Polwatthamodara	N5°57'18.5"	E80°27'18.5"	11span RC	Without bearing	162	99.10	2.04	9.01	8.10	0.51	2.67	Hearing	D
43	Polwattha Modara Small Bridge	Mirisssa	N5°57'51.1"	E80°27'21.9"	1span RC	Without bearing	202	7.29	1.15	7.29	10.65	0.65	4.20	Hearing	D
44	Udappala Bridge	Mirisssa	N5°56'40.9"	E80°27'37.8"	1span RC	Without bearing	33	15.80	0.97	15.80	10.22	1.05	4.03	Hearing	B
45	Ma-1	Matara	N5°56'19.8"	E80°29'01.4"	1span RC	Rubber pad type	107	7.88	1.72	7.88	10.64	0.57	3.85	Hearing	A
46	New Bridge	Matara	N5°56'48.5"	E80°32'23.8"	1span RC	Without bearing	57	12.12	1.41	12.12	7.56	0.37	3.27	Hearing	D
47	Matara Bridge	Matara	N5°56'43.3"	E80°32'55.5"	3span PC	Rubber pad type	135	112.40	3.19	22.48	16.24	0.82	6.26	Hearing	D
48	Wellaweds Bridge	Dewinawara	N5°55'53.1"	E80°34'57.0"	2span RC	Without bearing	25	19.79	1.59	-	7.94	0.84	5.68	Hearing	B
49	Th-1	Thalalla	N5°55'50.5"	E80°37'29.7"	1span RC	Without bearing	41	2.20	0.74	2.20	9.55	0.47	4.26	Hearing	D
50	Kot-1	Kottegoda	N5°55'58.9"	E80°38'22.5"	1span RC	Without bearing	-	11.46	1.65	11.46	12.20	0.45	2.71	Hearing	D
51	Bathigawa Bridge	Bathigawa	N5°55'40.3"	E80°40'41.4"	1span RC	Without bearing	70	15.90	3.97	15.90	9.73	0.99	2.00	Hearing	D
52	Di-1	Dikwella	N5°55'37.9"	E80°40'53.3"	1span RC	Without bearing	64	2.22	0.51	2.22	11.05	0.38	3.33	Hearing	D
53	Dikwella Bridge	Dikwella	N5°55'31.3"	E80°41'52.9"	3span RC	Rubber pad type	66	55.96	2.12	18.65	15.70	0.98	5.85	Hearing	C
54	Ta-1	Tangalla	N6°00'59.7"	E80°47'14.4"	1span RC	Without bearing	37	3.81	2.58	3.81	9.69	0.51	3.09	Hearing	D
55	Kirambo Bridge	Tangalla	N6°01'43.2"	E80°47'41.9"	1span steel truss	Without bearing	114	25.47	5.51	25.47	9.46	-	7.54	Hearing	B
56	Ha-1	Hambantota	N6°01'13.9"	E81°03'59.0"	1span RC	Without bearing	102	4.05	2.31	4.05	9.82	0.59	-	-	D
57	Bomuwatya Bridge	Hambantota	N6°00'53.0"	E81°07'34.7"	1span RC	Without bearing	158	17.16	2.93	17.16	10.05	1.04	12.37	Hearing	B
58	H1	Hambantota	-	-	1span RC	Without bearing	-	11.80	3.00	11.80	2.30	0.50	8.00	Hearing	A
59	T1	Tincomalee	-	-	21span PC	Unknown	-	147.00	3.50	7.00	7.00	0.80	6.00	Hearing	B
60	T2	Tincomalee	-	-	6span PC	Unknown	-	48.00	3.20	8.00	8.00	0.80	8.00	Hearing	B

Table 2 Damage pattern of a bridge structure due to a tsunami

Rank	Damage mode
A	Washout and fall-down of a deck
B	Movement of a deck Damage to an abutment Scouring and erosion of a soil embankment around an abutment
C	Damage to a deck attachment such as bridge railings
D	No damage

tion depth is defined as that of the height from the still water surface level under a subject bridge to the inundation line marked on a house located around a subject bridge where the inundation line could be identified and measured during the survey. However, when it could not be, the value of the inundation depth is defined as that of the height from the still water surface level under a subject bridge to the inundation depth level over the bridge surface on the basis of the associated information by hearings from inhabitants living in houses around a subject bridge.

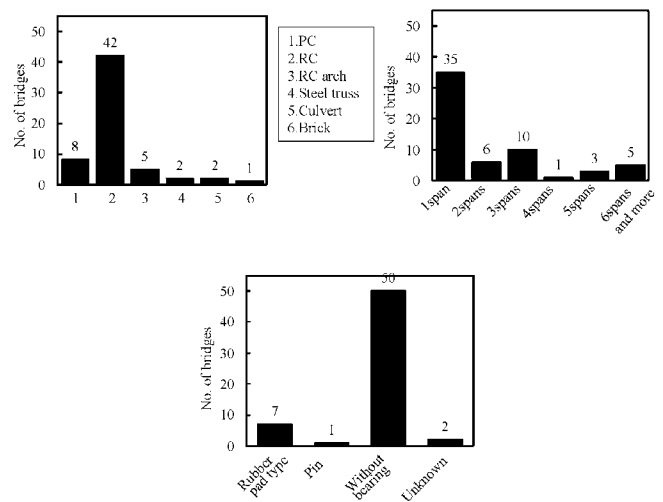


Fig. 2 Structural type, span, and bearing type of subject bridges in Sri Lanka

Because the values of the inundation depth are those dependent on the tide level at the site of a subject bridge at the time of day of the field survey, the values of the inundation depth were adjusted to those on December 26th, 2004, using the method of Tsuji et al. (2005), as follows (Fig. 4):

$$H = a + b - c \tag{6}$$

where H is the inundation depth adjusted as the value on December

26th, 2004, a is the height from the still water surface level under a subject bridge to the inundation depth level over the subject bridge at the time of day of the field survey, b is the difference in height between the still water surface level at the time of day of the field survey and the minimum still water surface level, and c is the difference in height between the still water surface level on December 26th, 2004 and the minimum still water surface level. a is obtained directly from the survey data, and b and c are the values of astronomical tide levels in Colombo and Galle numerically computed by Tsuji et al. (2005). In Sri Lanka, these values are obtained at only two sites, Colombo and Galle, and then, to adjust the value of the inundation depth at subject bridges located near Colombo (bridge nos. 1 to 23 in Table 1), the values of b and c are used as those of astronomical tide levels in Colombo, whereas to adjust the value at subject bridges located near Galle (bridge nos. 24 to 58 in Table 1), the values of b and c are used as those of astronomical tide levels in Galle. However, two data of bridge nos. 59 and 60 in Trincomalee associated with inundation depth are not adjusted by Eq. (6) because the two sites of bridge nos. 59 and 60 are far from either Colombo or Galle. From the adjustment, Fig. 5 shows the inundation depth at the sites of the subject bridges, accompanying related data collected by Tomita et al. (2005).

(2) DAMAGE DATA OF BRIDGE STRUCTURES IN SUMATRA

Damage data of bridge structures in the northwest of Sumatra Island in Indonesia, collected by the field survey team organized jointly by members from the Japan Society of Civil Engineers (JSCE) and the Japan Association of Earthquake Engineering (JAEE) in the summer of 2006 (JSCE and JAEE field survey

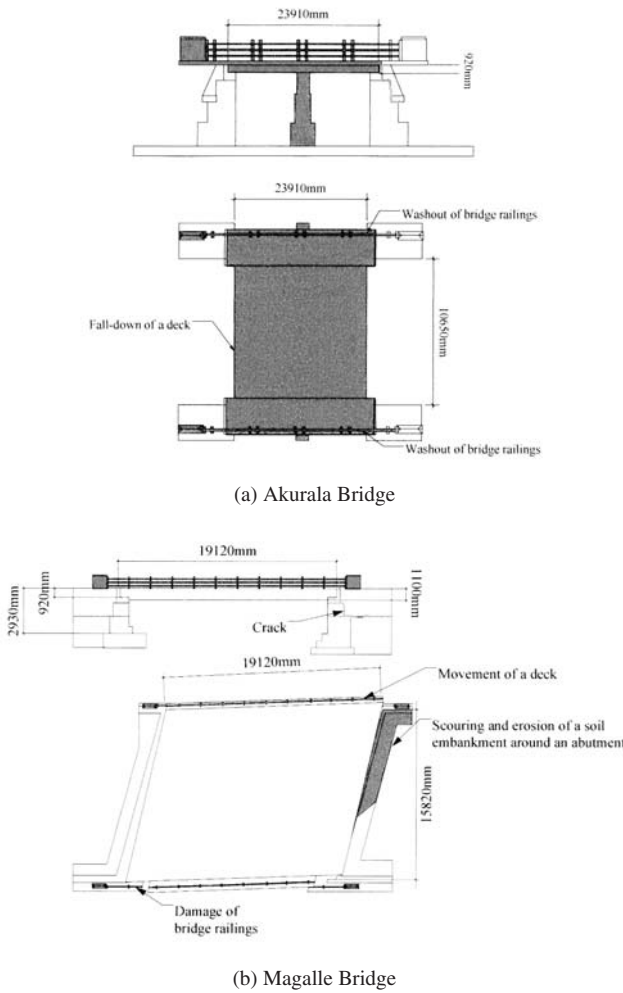


Fig. 3 Schematic view of affected bridges

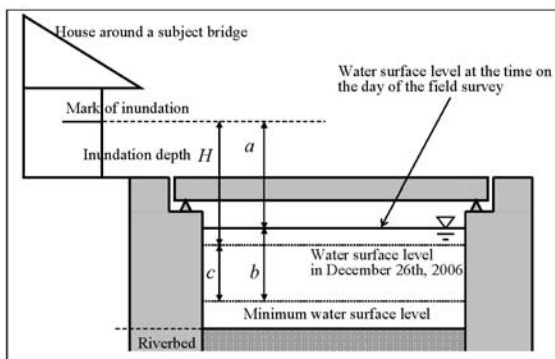


Fig. 4 Definition of inundation depth of a subject bridge in Sri Lanka

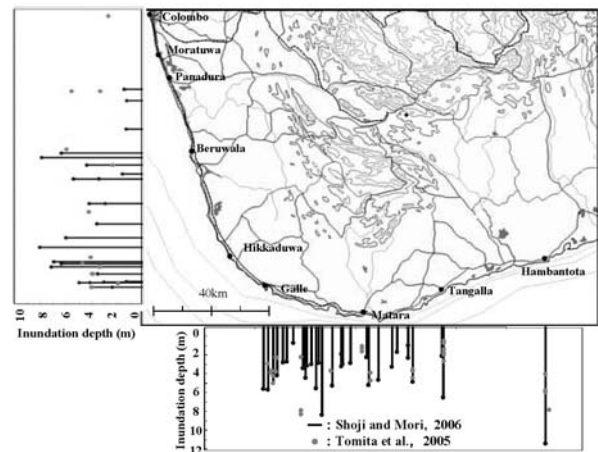


Fig. 5 Analyzed data associated with inundation depth at the sites of subject bridges in Sri Lanka

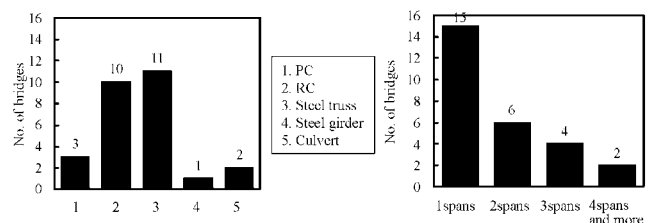


Fig. 6 Structural type and span of subject bridges in Sumatra

team), as well as data of Sri Lanka, are used for structural fragility analysis. **Table 3**, like **Table 1**, shows the data associated with structural characteristics and damage to 27 subject bridges in Sumatra due to the tsunami. The context of the data regarding the bridges in Sumatra in **Table 3** (Sumatra data) is almost same as that regarding the bridges in Sri Lanka in **Table 1** (Sri Lanka data). However, the data associated with bearing type, distance from the coastline to a subject bridge, and height from the still water surface level under the bridge to the deck are not collected in the Sumatra data. **Fig. 6** shows the structural type and span of subject bridges in the Sumatra data. In assessing the Sumatra data, not the inundation depth but the inundation height around a subject bridge is used as the quantitative index to present a tsunami wave load on a bridge structure in mechanics. These data are measured by Tsuji et al. (2005) and Fujima et al. (2006). **Fig. 7** shows the location of subject bridges and information on inundation height and tsunami runup height in the northwest of Sumatra.

3.2 FRAGILITY ANALYSIS

(1) DEVELOPMENT OF FRAGILITY CURVES

Now, fragility curves both in the Sri Lanka data and the Sumatra data are developed by the modification of Eq. (5) as previously described in the Chapter 2. Fifty-eight data among 60 in the Sri Lanka data, in which 2 data of unaffected bridges are included, and 17 data among 27 in the Sumatra data, with the information on inundation height around subject bridges, are used for fragility analysis.

Cumulative damage probability P_c^i (i =rank A ~ rank D) of a bridge structure due to a tsunami wave load, by which the damage to affected bridges is classified as rank A to rank D as shown in **Table 2**, is assumed to be the same as failure probability P_f of a

bridge structure due to a tsunami, and random variable Z , which describes the relationship between bridge resistance C with bridge

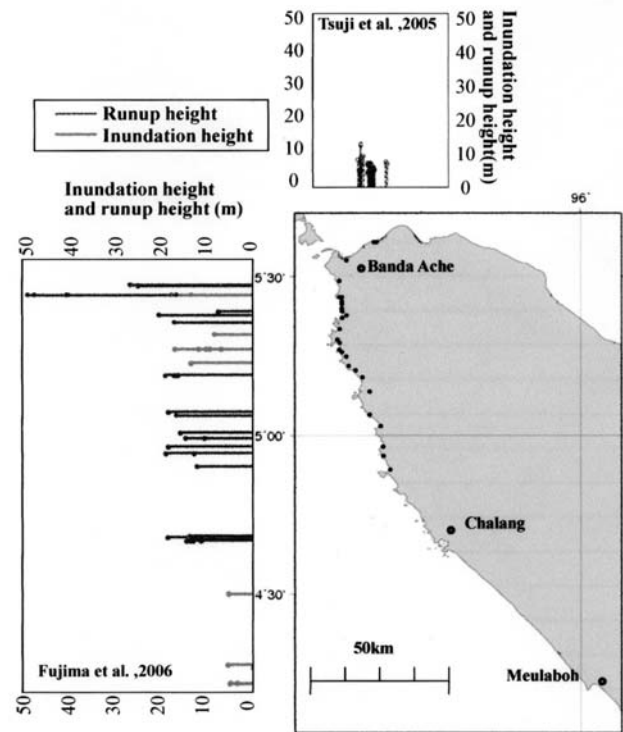


Fig. 7 Location of subject bridges and analyzed data associated with inundation height and tsunami runup height in the northwest of Sumatra

Table 3 Structural characteristics and failure mode of subject bridges, and data of inundation height and runup height around subject bridges in Sumatra

Number	Name of bridge	District	Latitude	Longitude	Structural type	Total length of deck (m)	Distance from water surface to deck (m)	Length of span(m)	Width of deck (m)	Height of deck (m)	Inundation(I) or Runup(R)	Inundation height (m)	Damage rank	Reference of tsunami height
1	Ulee Lheue Bridge	Banda Ache	N5°33'27.2"	E95°17'02.7"	3span PC	68.55	2.80	22.85	7.90	1.27	I	12.20	B	Tsuji, et al.
2	-	Banda Ache	N5°36'07.1"	E95°20'51.5"	2span RC	47.80	3.15	23.90	2.60	1.40	I	7.12	C	Tsuji, et al.
3	Out River Bridge	Banda Ache	N5°36'07.5"	E95°20'49.9"	10span RC	304.52	-	30.68	-	-	I	7.12	A	Tsuji, et al.
4	Kr.Raba Bridge	Lho-Nga	N5°28'12.2"	E95°14'35.9"	2span steel truss	69.36	1.31	34.68	7.00	-	I	18.38	A	Tsuji, et al.
5	Kr.Ritling Bridge	Leupung	N5°25'27.8"	E95°14'35.9"	2span RC	26.20	1.40	13.10	7.73	0.72	I	20.50	C	Tsuji, et al.
6	-	Leupung	N5°25'17.8"	E95°14'40.0"	1span RC	10.04	-	10.04	7.50	0.20	I	28.61	B	Tsuji, et al.
7	-	Leupung	N5°25'25.6"	E95°14'47.3"	1span RC	3.00	1.00	3.00	7.50	-	R	21.57	D	Tsuji, et al.
8	-	Leupung	N5°24'54.4"	E95°14'55.2"	1span RC	3.00	1.00	3.00	7.50	-	I	17.04	D	Tsuji, et al.
9	-	Leupung	N5°24'08.3"	E95°15'16.7"	1span RC	3.00	1.00	3.00	7.50	-	I	14.83	D	Tsuji, et al.
10	Gantang Pirak Bridge	Leupung	N5°23'13.1"	E95°15'19.3"	1span steel truss	25.00	2.00	25.00	8.83	-	I	22.45	A	Tsuji, et al.
11	Kr.Ihok Kaca Bridge	Leupung	N5°22'29.0"	E95°15'18.8"	Steel truss RC	81.00	3.30	62.00 19.00	9.73 9.73	- 0.80	I	13.08	A	Tsuji, et al.
12	Kr.Peulot Bridge	Leupung	N5°21'53.9"	E95°14'57.1"	1span steel truss	40.00	2.00	40.00	7.00	-	R	20.54	A	Fujima, et al.
13	Alue Tingaeuen Bridge	Leupung	N5°18'55.9"	E95°14'37.8"	3span culvert	-	-	-	-	-	-	-	C	-
14	Lam Ilie Bridge	Leupung	N5°17'10.5"	E95°14'37.2"	1span steel truss	35.00	2.00	-	6.00	-	I	8.45	A	Fujima, et al.
15	Kr.Lhong I Bridge	Gleeburk	N5°17'01.1"	E95°14'49.2"	2span steel truss	80.00	7.00	40.00	7.00	-	I	8.45	D	Tsuji, et al.
16	Kr.Mop Bridge	Gleeburk	N5°15'50.4"	E95°15'00.8"	3span culvert	12.00	-	-	-	-	I	9.52	C	Fujima, et al.
17	Lueng Ie Bridge	Gleeburk	N5°15'02.3"	E95°15'10.4"	1span RC	19.10	2.40	19.10	10.20	1.00	I	9.52	B	Fujima, et al.
18	Lam Ara Bridge	Gleeburk	N5°14'11.4"	E95°15'29.2"	1span RC	19.13	4.00	18.00	7.00	1.10	I	9.52	B	Fujima, et al.
19	Kr.Cuntuem Bridge	Gleeburk	N5°12'30.4"	E95°16'18.1"	1span steel girder	20.80	-	20.80	9.00	0.80	I	13.55	B	Fujima, et al.
20	Kr.Peudeng Bridge	Gleeburk	N5°11'56.1"	E95°17'02.1"	2span steel truss	83.00	5.00	41.50	7.00	-	I	13.55	A	Fujima, et al.
21	Kr.Lhong Kareubg Bridge	Ujung Muloh	N5°10'06.7"	E95°18'33.2"	1span steel truss	30.35	-	30.35	7.00	1.10	R	17.53	A	Fujima, et al.
22	Kr.Sapek	Ujung Muloh	N5°07'45.6"	E95°20'26.3"	1span steel truss	35.00	5.00	35.00	8.62	-	-	-	D	-
23	Kr.Lam Beusou Bridge	Lho kluet	N5°03'04.0"	E95°20'20.4"	6span PC	192.00	-	32.00	7.20	1.68	R	18.47	A	Fujima, et al.
24	Kuala Unga Bridge	Lho kluet	N5°00'44.0"	E95°21'56.5"	3span PC	95.90	6.00	32.00	6.00	-	R	15.88	A	Fujima, et al.
25	Alue Gemenatuet Bridge	Lho kluet	N4°56'55.3"	E95°22'16.4"	1span RC	6.50	2.00	6.50	6.80	-	R	18.54	A	Fujima, et al.
26	Kr.No Bong Bridge	Lho kluet	N4°55'17.4"	E95°23'14.1"	1span steel truss	61.00	3.00	61.00	6.00	-	R	19.08	A	Fujima, et al.
27	Kr.Krak Mong Bridge	Lho kluet	N4°52'54.7"	E95°24'12.8"	1span steel truss	45.00	2.00	45.00	6.00	-	R	12.47	A	Fujima, et al.

response R , is assumed to be the variable to present a tsunami wave load,

$$P_c^i = \int_0^z \frac{1}{\sqrt{2\pi} \cdot \sigma_Y \cdot z} \exp\left\{-\frac{1}{2} \left(\frac{\ln z - \mu_Y}{\sigma_Y}\right)^2\right\} dz \quad (7)$$

where μ_Y and σ_Y are mean and standard deviation of random variable Y , which is defined as the logarithm of random variable Z : $Y = \ln Z$. z means the value of Z . In assessing the Sri Lanka data, an inundation depth H (Fig. 4) is idealized as tsunami wave load Z , whereas in assessing the Sumatra data, an inundation height H is idealized as tsunami wave load Z , as shown in Fig. 8. In addition, we have the relationship between μ_Y and the median of Z , \hat{m}_Z , and that between σ_Y and the coefficient of variation of Z , V_Z , as follows:

$$\begin{aligned} \mu_Y &= \ln \hat{m}_Z \\ \sigma_Y^2 &= \ln(1 + V_Z^2) \end{aligned} \quad (8)$$

Tables 4 and 5 show the frequency of damage rank i ($i = \text{rank A} \sim \text{rank D}$) of subject bridges d^i , its cumulative frequency d_c^i , and cumulative damage probability P_c^i with the function of tsunami wave load Z in the Sri Lanka data and the Sumatra data, respectively. The value of the section in which the range of inundation depth is divided is 1 m in the Sri Lanka data, whereas it is 4 m in the Sumatra data, considering the coefficient of determination to obtain the linear regression lines between $\Phi^{-1}(P_c^i)$ (Φ means the standard

normal distribution function) and $\ln z$ as described below.

The values of P_c^i are transformed into those of $\Phi^{-1}(P_c^i)$ by the inversion of standard normal distribution function Φ , and those are defined as observed data $\Phi_{obs}^{-1}(P_c^i)$. Then, linear regression lines $\Phi_{fit}^{-1}(P_c^i)$ to idealize the relation between observed data $\Phi_{obs}^{-1}(P_c^i)$ (vertical direction: y -axis) and $\ln z$ (horizontal direction: x -axis) are derived by the method of least squares, as shown in Figs. 9 and 10, as follows:

$$\Phi_{fit}^{-1}(P_c^i) = \frac{\ln z - \mu_Y}{\sigma_Y} = \frac{1}{\sigma_Y} \ln z - \frac{\mu_Y}{\sigma_Y} \quad (9)$$

Tables 6 and 7 show the values of the y -intercept ($-\mu_Y/\sigma_Y$) and x y -inclination ($1/\sigma_Y$) derived from Figs. 9 and 10, the coefficient

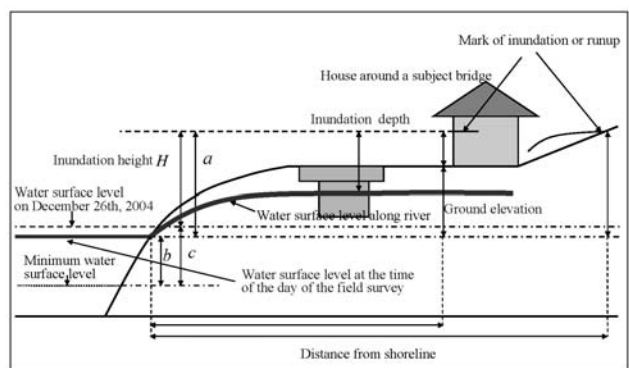


Fig. 8 Definition of a tsunami wave load on a subject bridge

Table 4 Frequency of damage rank i of subject bridges d^i , its cumulative frequency d_c^i , and cumulative damage probability P_c^i based on the Sri Lanka data

Inundation depth(m) Z	Frequency (No. of bridges)				Cumulative frequency (No. of bridges)				Cumulative damage probability P_c^i			
	A	B	C	D	A	A+B	A+B+C	A+B+C+D	A	A+B	A+B+C	A+B+C+D
0~1	0	0	0	0	0	0	0	0	-	-	-	-
1~2	0	0	0	0	0	0	0	0	-	-	-	-
2~3	0	1	0	6	0	1	1	7	0.000	0.143	0.143	1.000
3~4	0	0	0	4	0	0	0	4	0.000	0.000	0.000	1.000
4~5	2	4	0	7	2	6	6	13	0.154	0.462	0.462	1.000
5~6	1	3	1	5	1	4	5	10	0.100	0.400	0.500	1.000
6~7	0	3	2	1	0	3	5	6	0.000	0.500	0.833	1.000
7~8	2	2	2	4	2	4	6	10	0.200	0.400	0.600	1.000
8~9	2	2	0	1	2	4	4	5	0.400	0.800	0.800	1.000
9~10	1	0	0	0	1	1	1	1	1.000	1.000	1.000	1.000
10~11	0	0	0	1	0	0	0	1	0.000	0.000	0.000	1.000
11~12	0	0	0	0	0	0	0	0	-	-	-	-
12~13	0	0	0	0	0	0	0	0	-	-	-	-
13~14	1	0	0	0	1	1	1	1	1.000	1.000	1.000	1.000
Summation	9	15	5	29	9	24	29	58	-	-	-	-

Table 5 Frequency of damage rank i of subject bridges d^i , its cumulative frequency d_c^i , and cumulative damage probability P_c^i based on the Sumatra data

Inundation height(m) Z	Frequency (No. of bridges)				Cumulative frequency (No. of bridges)				Cumulative damage probability P_c^i			
	A	B	C	D	A	A+B	A+B+C	A+B+C+D	A	A+B	A+B+C	A+B+C+D
~3	0	0	0	0	0	0	0	0	-	-	-	-
3~7	0	0	0	0	0	0	0	0	-	-	-	-
7~11	2	2	2	1	2	4	6	7	0.286	0.571	0.857	1.000
11~15	2	2	0	1	2	4	4	5	0.400	0.800	0.800	1.000
15~19	1	0	0	1	1	1	1	2	0.500	0.500	0.500	1.000
19~23	1	0	1	0	1	1	2	2	0.500	0.500	1.000	1.000
23~27	0	0	0	0	0	0	0	0	-	-	-	-
27~	0	1	0	0	0	1	1	1	0.000	1.000	1.000	1.000
Summation	6	5	3	3	6	11	14	17	-	-	-	-

Table 6 Mean μ_y , standard deviation σ_y , and median \hat{m}_z of inundation depth Z based on the Sri Lanka data

Damage rank	A	A+B	A+B+C
Inclination	0.88	0.97	1.15
Intercept	-2.46	-1.73	-1.74
Coefficient of determination	0.79	0.83	0.80
Mean μ_y	2.80	1.78	1.51
Standard deviation σ_y	1.14	1.03	0.87
Median \hat{m}_z	16.39	5.93	4.52

Table 7 Mean μ_y , standard deviation σ_y , and median \hat{m}_z of inundation height Z based on the Sumatra data

Damage rank	A
Inclination	0.7169
Intercept	-2.112
Coefficient of determination	0.94
Mean μ_y	2.95
Standard deviation σ_y	1.39
Median \hat{m}_z	19.03

of determination when adopting the method of least squares. Mean μ_y and standard deviation σ_y derived from the y-intercept and x y-inclination adopting Eq. (9) and median \hat{m}_z of tsunami wave load Z derived from Eq. (8) are also shown in **Tables 6** and **7**. Hence, all parameters to model cumulative damage probability P_c^i shown in Eq. (7) are determined, and the fragility curves associated with cumulative damage probability P_c^i of a bridge structure against tsunami wave load Z can be developed as shown in **Figs. 11** and **12**.

In **Fig. 12**, only the fragility curve of rank A is derived because based on the Sumatra data, the number of data related to damage of rank B and rank C is not sufficiently obtained for the linear regression analysis. **Figs. 11** and **12** shows the structural fragility of the total subject bridges based on 58 data in the Sri Lanka data and 17 data in the Sumatra data; the curves indicate the general fragility trends of a bridge structure and contain information associated with various types of structures. Therefore, in the following, the fragility curve that presents the specific fragility trends of a single-spanned reinforced concrete bridge without bearings, based on the Sri Lanka data, referring to **Fig. 2**, is derived as shown in **Fig. 13**.

(2) TRENDS OF TSUNAMI FRAGILITY OF A BRIDGE STRUCTURE

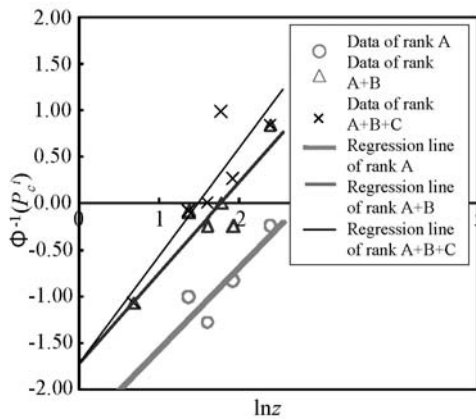


Fig. 9 Relation between the data of $\Phi_{obs}^{-1}(P_c^i)$ and $\ln z$ based on the Sri Lanka data and regression lines $\Phi_{fit}^{-1}(P_c^i)$

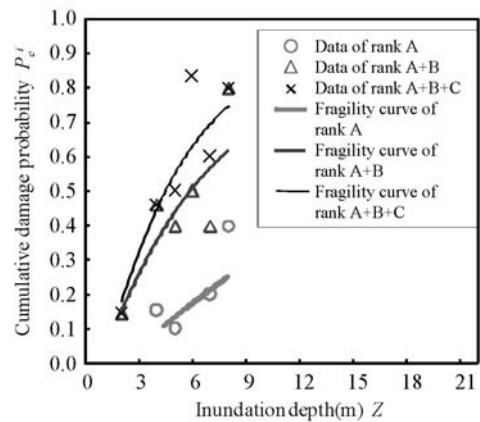


Fig. 11 Fragility curve of a bridge structure due to a tsunami based on the Sri Lanka data

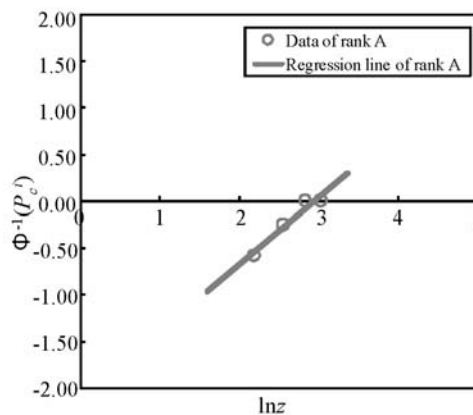


Fig. 10 Relation between the data of $\Phi_{obs}^{-1}(P_c^i)$ and $\ln z$ based on the Sumatra data and regression line $\Phi_{fit}^{-1}(P_c^i)$

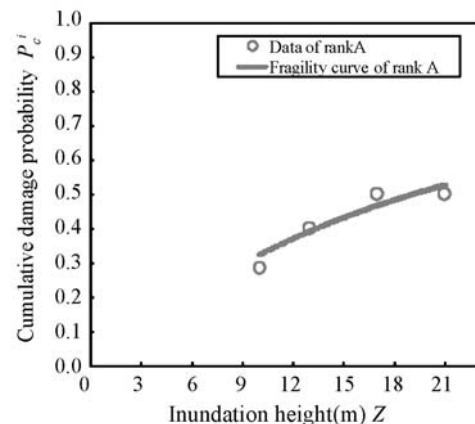


Fig. 12 Fragility curve of a bridge structure due to a tsunami based on the Sumatra data

From **Fig. 11**, damage probability $P^A (=P_c^A)$ of rank A, which means washout and fall-down of a deck, becomes nearly 0.1 when the inundation depth is 4 m, whereas the value of P^A increases from 0.2 to 0.25 when the inundation depth increases from 6 m to 8 m. Damage probability $P^B (=P_c^B - P_c^A)$ of rank B, which means movement of a deck or damage to an abutment due to scouring and erosion, becomes nearly 0.3 when the inundation depth is 4 m, whereas the value of P^B increases from 0.3 to 0.35 when the inundation depth increases from 6 m to 8 m.

Compared with the trend of P^A in **Fig. 11**, derived by the use of all the data among the Sri Lanka data (all bridge data), the trend of P^A in **Fig. 13**, derived by the use of only the data associated with a single-spanned reinforced concrete bridge without bearings (single-spanned bridge data), becomes different; the value of P^A based on the single-spanned bridge data becomes larger than that based on all bridge data when the inundation depth approaches a value from 6 m to 8 m, although the values of P^A based on both the single-spanned bridge data and on all bridge data are almost same when the inundation depth is 4 m. This indicates that a single-spanned reinforced concrete bridge without bearings subjected to a tsunami wave load is more fragile compared to other types of bridge structure. One explanation for this may be that drag force $Q_d^{I span}$ against a tsunami wave induced in a deck of a single-spanned bridge becomes smaller than the $Q_d^{M span}$ induced in decks of a multi-spanned bridge, supposing that tsunami wave velocity v is almost same when inundation depth Z is the same in this analysis based on the Sri Lanka data. Now, drag force Q_d is derived as follows:

$$Q_d = \frac{1}{2} \rho_w C_d A v^2 \quad (10)$$

where ρ_w is the mass of sea water in a unit volume, C_d is the drag coefficient, and A is the section area of a deck subjected to a tsunami wave. The drag coefficient of a deck of a single-spanned bridge, $C_d^{I span}$, and that of a deck of a multi-spanned bridge, $C_d^{M span}$, could be assumed to be almost the same, and the section area of a deck of a single-spanned bridge subjected to a tsunami wave, $A^{I span}$, becomes smaller than that of a deck of a multi-spanned bridge subjected to a tsunami wave, $A^{M span}$; hence, from Eq. (10), $Q_d^{I span}$ becomes smaller than $Q_d^{M span}$, supposing that tsunami wave velocity v is almost same.

On the other hand, in **Fig. 12**, which is the case based on the Sumatra data, damage probability P^A of rank A when the inundation height becomes more than 9 m is clarified because not inundation depth but inundation height is used as the index of a tsunami wave load. From **Fig. 12**, damage probability P^A of rank A becomes nearly 0.4 when the inundation height is 12 m, whereas P^A increases to nearly 0.5 when the inundation height increases to 20 m; this inundation height level corresponds to an extreme tsunami wave load, and it has high possibility of causing catastrophic damage to a bridge structure.

(3) FAILURE MECHANISM OF A BRIDGE STRUCTURE BY A TSUNAMI WAVE LOAD

Now, we will hypothesize that the mechanism of the tsunami wave load on a bridge structure is qualitatively divided into two mechanisms; the mechanism due to the flow induced by a tsunami wave (mechanism I) and that due to the impulsive pressure induced by a tsunami wave (mechanism II), as shown in **Fig. 14**. It might be considered that not mechanism I but mechanism II occurs when a tsunami wave load becomes extremely large compared to the capacity of resistance of a bridge structure, for instance, when the inundation depth or inundation height becomes extremely large.

Such a hypothesis makes it possible for the fragility curves from **Fig. 11** and **Fig. 13** based on the Sri Lanka data to result from mechanism I, whereas the fragility curve from **Fig. 12** based on the Sumatra data results from mechanism II. Examining it in detail, a tsunami wave load within the range 5-m to 10-m inundation depth corresponds to that on a bridge structure associated with mechanism I, whereas a tsunami wave load beyond the range of 10-m inundation height and approaching a 20-m inundation height corresponds to that associated with mechanism II. The tsunami wave load on mechanism I causes the movement of a deck following the washout and fall-down of a deck, which results in 'major' damage to a bridge structure of either rank B or rank A at its worst, whereas that on mechanism II causes the direct and catastrophic washout

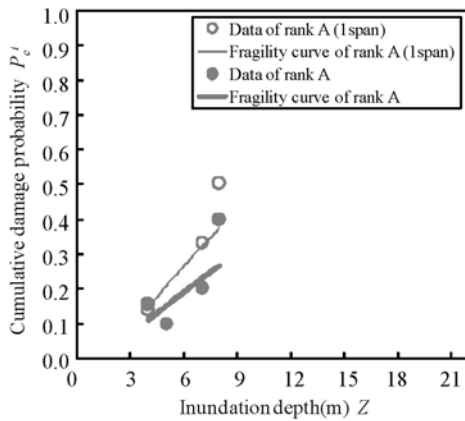


Fig. 13 Fragility curve of a bridge structure due to a tsunami based on the data associated with a single-spanned reinforced concrete bridge without bearings among the Sri Lanka data

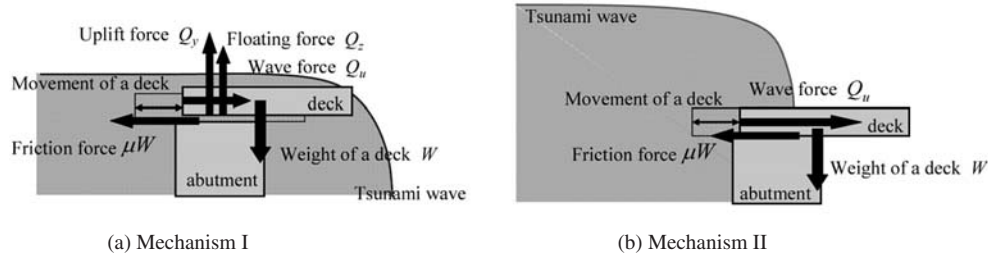


Fig. 14 Mechanism of the tsunami wave load on a bridge structure

and fall-down of a deck and columns, which results in 'severe' damage of rank A. However, because there is no direct and independent evidence to decide the above matter, further numerical and experimental studies will be performed to prove our hypothesis.

4. CONCLUSIONS

In this study, the structural fragility of a bridge structure due to a tsunami wave load was evaluated, quantitatively analyzing the damage data of bridge structures in Sri Lanka and in Indonesia due to the 2004 Giant Tsunami in the Indian Ocean, which are on basis of 58 data on Sri Lanka (Sri Lanka data) and 17 data on Sumatra (Sumatra data). Assessing the data and classifying the tsunami damage to a bridge structure into washout and fall-down of a deck (rank A), movement of a deck or damage to an abutment due to scouring and erosion (rank B), minor damage to a deck attachment such as bridge railings (rank C), to no damage (rank D), the relation between the probability of tsunami damage to a bridge structure with a tsunami wave load such as inundation depth and inundation height is clarified with the development of fragility curves. From the analysis, the following conclusions are deduced.

- 1) From the fragility curves derived based on the Sri Lanka data dealing with a 'major' tsunami wave load on a bridge structure, which means an inundation depth level within 10 m, damage probability P^A or P^B of rank A or rank B becomes nearly 0.2 to 0.3 when the inundation depth comes within 5 m, whereas the value of P^A or P^B increases from 0.35 to 0.4 when the inundation depth approaches a value close to the 10-m order; it might cause the failure mode of a bridge structure due to the flow induced by a tsunami wave.
- 2) From the fragility curves derived based on the Sumatra data dealing with a 'severe' tsunami wave load on a bridge structure, which means an inundation height level ranging from 10 m to 20 m, damage probability P^A of rank A becomes nearly 0.4 when the inundation height reaches the value beyond 10 m, whereas P^A increases to nearly or more than 0.5 when the inundation height approaches a value of 20 m; it might cause the failure mode of a bridge structure due to the impulsive pressure induced by a tsunami wave.

ACKNOWLEDGEMENTS

This research was sponsored by the Ministry of Education, Culture, Sports, Science and Technology (MEXT) under a grant provided as Special Coordination Funds for Promoting Science and Technology, associated with the 2004 Giant Tsunami in the Indian Ocean 'Restoration Program from Giant Earthquakes and Tsunamis' (leader, Professor T. Kato at University of Tokyo, Professor H. Iemura at Kyoto University, and Professor O. Murao at University of Tsukuba). The authors deeply appreciate research information and valuable assistance associated with the field survey in Sri Lanka, provided by Mr. G. N. Paranavithana at Natural Resources Management Services (Pvt.), Ltd. in Sri Lanka, Mr. N. Rupasinghe at the Central Engineering Consultancy Bureau in Sri Lanka, Dr. S. Herath at the United Nations University, and Professor K. Meguro at the University of Tokyo. The authors are also deeply grateful for research information and valuable assis-

tance associated with the field survey on Sumatra in Indonesia, provided by the members of the field survey team organized by the Japan Society of Civil Engineers (JSCE) and the Japan Association of Earthquake Engineering (JAE) (leader, Professor M. Miyajima at Kanazawa University, Professor K. Fujima at National Defense Academy of Japan, Professor K. Kosa at the Kyushu Institute of Technology, and Professor H. Matsutomi at Akita University).

REFERENCES

- Asakura, R., Iwase, K., Ikeya, T., Takao, M., Kaneto, T., Fujii, N. and Omori, M., 2000. An Experimental Study on Wave Force Acting on On-Shore Structures due to Overflowing Tsunamis, *Proceedings of Coastal Engineering, JSCE*, 47, 911-915 (in Japanese).
- Fujima, K. et al., 2006. Tsunami Measurement Data Compiled by IUGG Tsunami Commission, <http://www.nda.ac.jp/~fujima/TMD/>.
- Fukuoka, S., Kawashima, M., Yokoyama, H. and Mizuguchi, M., 1997. Experimental Study of Hydrodynamic Forces Acting on a Group of Buildings, *Journal of Hydroscience and Hydraulic Engineering, JSCE* 41, 693-698 (in Japanese).
- Hatori, T., 1984. On the Damage to Houses due to Tsunamis, *Bulletin of the Earthquake Research Institute, University of Tokyo*, 59, 433-439 (in Japanese).
- Iemura, H., Pradono, M. H., and Takahashi, Y., 2005. Report on the Tsunami Damage of Bridges in Banda Aceh and Some Possible Countermeasures, *Proceedings of 28th Earthquake Engineering Symposium (CD-ROM), JSCE*.
- Iizuka, H. and Matsutomi, H., 2000. Damage due to the Flooding Flow of Tsunami, *Proceedings of Coastal Engineering, JSCE*, 47, 381-385 (in Japanese).
- Kosa, K., Uno, H., Miyajima, M., Ono, Y. and Hashimoto, T., 2006. Survey of Bridge Damage in the Sumatra Earthquake, *Proceedings of the Symposium on Recent Damaging Earthquakes around the World, Earthquake Damage Investigation Subcommittee, Earthquake Engineering Committee, JSCE*, 86-91 (in Japanese).
- Matsutomi, H. and Shuto, N., 1994. Inundation Depth due to a Tsunami and Damage of Houses, *Proceedings of Coastal Engineering, JSCE*, 41, 246-250 (in Japanese).
- Matsutomi, H. and Iizuka, H., 1998. Tsunami Current Velocity on Land and Its Simple Estimation Method, *Proceedings of Coastal Engineering, JSCE*, 45, 361-365 (in Japanese).
- Matsutomi, H. and Ohmukai, T., 1999. Laboratory Experiments on Fluid Force of Tsunami Flooded Flows, *Proceedings of Coastal Engineering, JSCE*, 46, 336-340 (in Japanese).
- Mizutani, S. and Imamura, F., 2000. Hydraulic Experimental Study on Wave Force of a Bore Acting on a Structure, *Proceedings of Coastal Engineering, JSCE*, 47, 946-950 (in Japanese).
- Shoji, G. and Mori, Y., 2006. Damage of Road Structures in Sri Lanka due to the 2004 Giant Tsunami in the Indian Ocean, *Proceedings of the 9th Symposium on Ductility Design Method for Bridges, JSCE* 221-224 (in Japanese).
- Shuto, N., 1993. Tsunami Intensity and Disasters, *Tsunamis in the World*, 197-216.
- Tomita, T., Arikawa, T., Yasuda, T., Imamura, F. and Kawata, Y., 2005. Field Survey around South West Coast of Sri Lanka of the December 26, 2004 Earthquake Tsunami Disaster of Indian Ocean, *Proceedings of Coastal Engineering, JSCE*, 52, 1406-1410 (in Japanese).
- Tsuji, Y., Namegaya, Y., and Ito, J., 2005. Astronomical Tide Levels along the Coasts of the Indian Ocean, <http://www.eri.u-tokyo.ac.jp/namegaya/sumatera/tide/index.htm>.
- Tsuji, Y., Matsutomi, H., Tanioka, Y., Nishimura, Y., Sakakiyama, T., Kamataki, T., Murakami, Y., Moore, A. and Gelfenbanm, G., 2005. The Distribution of the Tsunami Heights in Banda Aceh, <http://www.eri.u-tokyo.ac.jp/namegaya/sumatera/surveylog/eindex.htm>.
- Unjoh, S., 2005. Damage to Transportation Facilities, The Damage induced by Sumatra Earthquake and Associated Tsunami of December 26, 2004, <http://www.jsce.or.jp/committee/2004sumatra/report.htm>, *JSCE*, 66-76.
- USGS Earthquake Center, 2007. <http://earthquake.usgs.gov/eqcenter/eqinthenews/2004/usslav/>.